TÜBİTAK

Turkish Journal of Earth Sciences

http://journals.tubitak.gov.tr/earth/

Research Article

Turkish J Earth Sci
(2019) 28: 787-804
© TÜBİTAK
doi:10.3906/yer-1906-13

Late Holocene coseismic rupture and aseismic creep on the Bolvadin Fault, Afyon Akşehir Graben, Western Anatolia

Çağlar ÖZKAYMAK[1,2,*], Hasan SÖZBİLİR[3,4], Mertkan Osman GEÇİEVİ[5], İbrahim TİRYAKİOĞLU[6,2]

[1]Department of Geological Engineering, Faculty of Engineering, Afyon Kocatepe University, Afyon, Turkey
[2]Earthquake Research and Implementation Center of Afyon Kocatepe University, Afyon, Turkey
[3]Department of Geological Engineering, Faculty of Engineering, Dokuz Eylül University, İzmir, Turkey
[4]Earthquake Research and Implementation Center of Dokuz Eylül University, İzmir, Turkey
[5]The Graduate School of Natural and Applied Sciences, Afyon Kocatepe University, Afyon, Turkey
[6]Department of Geomatics Engineering, Faculty of Engineering, Afyon Kocatepe University, Afyon, Turkey

Received: 12.06.2019 • **Accepted/Published Online:** 20.08.2019 • **Final Version:** 07.11.2019

Abstract: The Bolvadin Fault, which forms one of the northern boundaries of the Afyon Akşehir Graben, creeps aseismically on the surface of earth and has not generated surface-rupture earthquakes during instrumental time. Our geological mapping and palaeoseismological studies reveal that the Bolvadin Fault is an approximately 2 km wide and 16 km long, dip-slip normal fault. It could generate earthquakes up to Mw 6.48 roughly every 1 ka and the latest surface-rupture event (M > 6) occurred 494 ± 45 years ago on the Bolvadin Fault. The throw over the past 5 Ma is measured as approximately 500 m according to relative positions of the basal unconformity of Pliocene clastics on both sides of the fault yielding a long-term average slip rate of 0.1 mm/year. Palaeoseismic trenching at two sites on the Bolvadin Fault document that the fault was reactivated by at least two linear morphogenic earthquakes during the past 2570 years. They probably occurred in 530 (AD) and 1525 ± 45 (AD). We also determined a mean late Holocene slip rate of about 0.64 mm/year at trench 1. Palaeoseismic data suggests that aseismic surface deformations (postseismic relaxation) which began developing after the 2002 Çay earthquakes (Mw: 6.3 and 6.0) follows the older surface rupture of the Bolvadin Fault.

Key words: Afyon–Akşehir Graben, Bolvadin Fault, palaeoseismology, slip rate

1. Introduction

Aseismic fault creep is the name for the slow, constant slippage that can occur on some active faults without a destructive earthquake occurring (e.g., Thatcher, 1979; Burtford and Harsh, 1980). This creeping behaviour happens on all kinds of faults (e.g., Nadeau and McEvilly, 1999; Lee et al., 2003; Titus et al., 2006; Hreinsdóttir and Bennett, 2009; Harris, 2017), but the most obvious and the easiest way to visualise it is on strike-slip faults such as San Andreas Fault (e.g., Schulz et al., 1982; Sieh and Williams, 1990), North Anatolian Fault (e.g., Çakır et al., 2005; Karabacak et al., 2011), and East Anatolian Fault (e.g., Ergintav et al., 2017), where opposite sides move sideways with respect to each other. In recent studies, aseismic movements were recorded on active normal faults in western Anatolia (e.g., Demirtaş et al., 2008; Koca et al., 2011; Özkaymak et al., 2014, 2017, 2018). One of them is the Bolvadin Fault which is located in the tectonically critical area of a microplate border where three megatectonic structures overlap, namely, the Akşehir–Simav Fault System (ASFS), and the northwestern (the Fethiye–Burdur Fault Zone) and northeastern (the Sultandağı Fault) outer borders of the Isparta Angle. These neotectonic structures separate the West Anatolia Graben Systems from the inner and outer Isparta Angle and the Northwest Anatolia transition zone forming the West Anatolian Extensional Province (Emre et al., 2018). Two destructive earthquakes leading to the development of surface ruptures in Maltepe and Çay regions, which are located in the central part of the Afyon–Akşehir Graben (AAG) and just south of Bolvadin, occurred on 3 February 2002 with magnitudes of 6.3 and 6.0, respectively (Özden et al., 2002; Emre et al., 2003; Yürür et al., 2003; Akyüz et al., 2006; Tan et al., 2008). Furthermore, about 2000 earthquakes with magnitudes between 2 and 4 (2000 to 2017) reported along the AAG (Özkaymak et al., 2017; Tiryakioğlu et al. 2018; KOERI, 2019) demonstrate the high seismic activity in this region.

The ASFS is made up of numerous fault segments trending NW–SE with an approximate total length of 400 km between Sındırgı to the west and Ilgın to the

* Correspondence: activetectonics@gmail.com

This work is licensed under a Creative Commons Attribution 4.0 International License.

east (Koçyiğit, 1984; Koçyiğit et al., 2000; Koçyiğit and Özacar, 2003, Özkaymak et al., 2017; Tiryakioğlu et al., 2018) (Figure 1). While the northwestern part of the ASFS consists of seven right lateral strike slip fault segments with an average length of 30 km each, the southeastern part is represented by the AAG, a major NW–SE-trending and approximately 130 km-long active depression area (Koçyiğit, 1984, Koçyiğit et al., 2000; Koçyiğit ve Özacar, 2003, Emre et al., 2011; Özkaymak et al., 2017; Duman et al., 2018;). The AAG is currently experiencing extension of about 4 mm/year (Aktuğ et al., 2009; Duman et al., 2018), most of which is associated with earthquakes on active normal faults with magnitudes between 5.7 and 6.3. Normal faults in the graben have lengths in the range of 12–29 km and could generate earthquakes with magnitudes up to 6.8 (Emre et al., 2018). Despite higher seismic activity and distinctive active tectonic features, there are limited trench-based palaeoseismological investigations along the ASFS which are fundamental for earthquake hazard analysis. The first and only published palaeoseismological record from the AAG was performed on the surface ruptures of 3 February 2002 Çay earthquakes (Mw:6.3 and 6.0) by Akyüz et al. (2006). They suggest the occurrence of two surface faults after 1150 AD in Maltepe and before 760 AD in Çay trenches (Akyüz et al., 2006). On the other hand, Duman et al. (2013) and Gürboğa (2013) conducted trench-based studies along the northwestern part of the ASFS. Duman et al. (2013) described Holocene activity with at least five events which are associated with lateral strike slip faulting on the Çaysimav and Şaphane segments. Gürboğa (2013) identified two events (in 990 AD and 1020 AD) on the surface rupture of the 1970 Gediz earthquake (Ms: 7.2) and estimated the recurrence interval on the Erdoğmuş Fault as 910 ± 40 years which was unique along the ASFS. However, none of them detail aseismic creep on the studied faults.

In this study, we present new palaeoseismic evidence for late Holocene activity of aseismic creeping on the Bolvadin Fault. In addition, we also include geologic mapping and trench observations by correlating with the precision level measurements of aseismic surface deformations (Tiryakioğlu et al., 2019) which has been developing on the Bolvadin Fault since the 2002 Çay earthquakes. To do this, we firstly introduce the seismotectonic setting of the region, then our findings (kinematic analysis and palaeoseismology) and their results, and finally we compare our results with the previous works.

2. Seismotectonic setting

Historical and instrumental earthquake records suggest the existence of a large number of linear morphogenic earthquakes (Caputo., 2005) that created surface ruptures

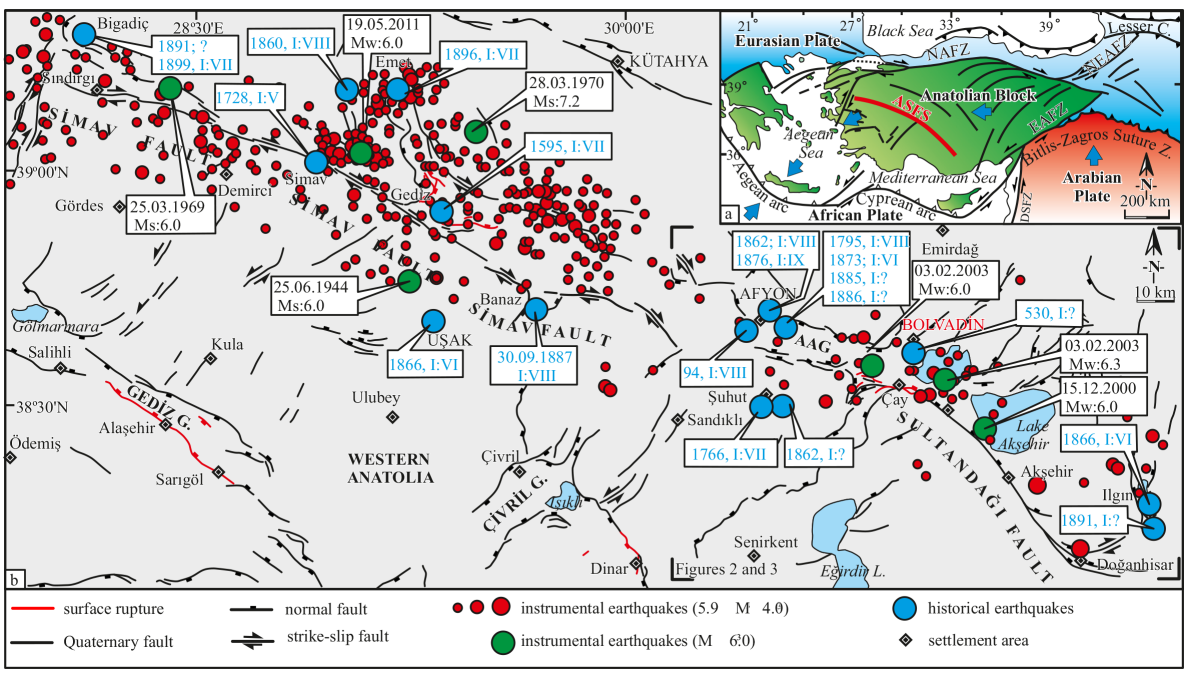


Figure 1. a) Tectonic outline of the eastern Mediterranean area (compiled from Kaymakcı, 2006 and Özkaymak, 2015). Abbreviations: ASFS, Akşehir–Simav Fault System; AAG, Afyon–Akşehir Graben; DSFZ, Dead Sea Fault Zone; EAFZ, East Anatolian Fault Zone; NAFZ, North Anatolian Fault Zone; NEAFZ, Northeast Anatolian Fault Zone. b) Seismotectonic map of the ASFS (faults are taken from Emre et al., 2011; earthquake data are taken from Duman et al., 2018)

in the AAG which was shaped by normal/oblique faults (Ergin et al., 1967; Soysal et al., 1981; Ambraseys, 1988, 2009; Ambraseys and Jackson, 1998; Özer, 2006; Tan et al., 2008; Tiryakioğlu et al., 2015; Özkaymak et al., 2017). These graben-bounding active faults are responsible for most of the earthquakes recorded in both historical and instrumental catalogues in the region (Özkaymak et al., 2017; Tiryakioğlu et al., 2018). According to Soysal et al. (1981), Afyonkarahisar was shaken by an earthquake in 94 AD with an intensity of VIII. They gave no further details. Ambraseys (2009) refers to an earthquake in 530 AD which destroyed the Phrygian town of Polybotus (Bolvadin). There is no further information about the event. A series of strong earthquakes were also reported in Şuhut and Afyonkarahisar in the second half of the 17th century (1766 or 1767 and 1795) with intensities of VII and VIII, respectively (Ergin et al., 1967; Soysal et al., 1981) (Figure 1, Table 1).

In 1862, a destructive earthquake with intensity VIII or X occurred south of Afyonkarahisar (Ergin et al., 1967; Shebalin et al., 1974; Soysal et al., 1981; Ambraseys and Jackson, 1998; Özer, 2006; Ambraseys, 2009; Duman et al., 2018). According to Ambraseys and Jackson (1998), the magnitude of the earthquake was 6.5. They also reported that this earthquake caused surface ruptures in Şuhut Plain. After the 1866 Ilgın and 1873 Afyonkarahisar earthquakes with intensity of VI, an event on May 13, 1876 caused extensive damage in Afyonkarahisar (Ergin et al., 1967; Soysal et al., 1981; Ambraseys, 2009). This was the most destructive earthquake affecting

Table 1. List of recorded historical and instrumental earthquakes in the Afyon–Akşehir Graben. References: (1) Soysal et al. (1981), (2) Duman et al. (2018), (3) Ambraseys (2009), (4) Ergin et al. (1967), (5) Shebalin et al. (1974), (6) Ambraseys and Jackson (1998), (7) Özer (2006), (8) Ambraseys (1988), (9) Pınar and Lahn (1952), (10) Taymaz and Tan (2001), (11) Tan et al. (2008), (12) KOERI (2019). Abbreviations: I, intensity; M, magnitude; R, references.

No	Date	Coordinate Lat.-Long.	Locality affected	I	M	R
1	94	38.75-30.50	Afyonkarahisar	VIII	?	1,2
2	530	38.65-31.10	Polybotus (Bolvadin)	?	?	3
3	1766 or 1767	38.50-30.50 or 38.53-30.55	Afyonkarahisar and Şuhut	VII	?	1,2,4,9
4	1795	38.76-30.50	Afyonkarahisar	VIII	?	1,2,4,9
5	1862, October 16 or 1862, November 3	38.80-30.50 38.50-30.30	Afyonkarahisar and Şuhut	VIII or X	6.1-6.5	1,2,3,4,5,6
6	1866	38.28-31.90 38.30-31.90	Ilgın	VI	?	1, 4,
7	1873, October 1	38.76-30.55	Afyonkarahisar	VI		1, 4,
8	1876, May 13	38.80-30.50 38.15-30.20	Afyonkarahisar	IX	6.7	1,2,4,5
9	1885, December 2 or 1885, November 28	38.75-30,55	Afyonkarahisar	?	?	2,3
10	1886, December 2	38.75-30,55	Afyonkarahisar	?	?	3
11	1911	38.5-29.5	Afyonkarahisar, Bolvadin, Çay, Akşehir	VIII	?	4, 7
12	1914	38.65-31.10	Bolvadin	VII	?	4
13	1921, September 26	38.38-31.75	Argıthanı, Akşehir	VIII	5.9 (M_s)	4,8,9
14	1928, November	38,76-30,53	Afyonkarahisar	V	?	4,7
15	1934, Jun 19	38.70-30.00	Afyonkarahisar, Uşak	VII	5.3-5.9	4
16	1934, November 19	38.76-30.53	Afyonkarahisar	V	?	4,7
17	1940, February 29	38.76-30.50	Afyonkarahisar	VII	6.0	4,
18	1941, January 29	38.76-30.50	Afyonkarahisar	V	?	4,7
19	1942, January 18	38.76-30.50	Afyonkarahisar	V	?	4,7
20	1946, February 21	38.35-31.78	Argıthanı, Akşehir	VIII	5.7 (M_s)	4,8
21	2000, December 15	38.59-31.16	Sultandağı	-	6.0	10,11
22	2002, February 3	38.58-31.25	Çay, Sultandağı	-	6.3	11,12
23	2002, February 3	38.69-30.84	Çay, Kadıköy	-	6.0	11,12

Afyonkarahisar city center. In the western part of the city, many houses collapsed with loss of life and aftershocks continued for 40 days (Ambraseys, 2009). According to the historical reports the maximum intensity was IX and a 6.7 magnitude was estimated (Soysal et al., 1981). Afyonkarahisar was shaken by a series of violent earthquakes between 1885 and 1886, though no sufficient information is available (Table 1).

The intraplate seismicity of the AAG concentrated in the middle section extending from east of Afyonkarahisar and Akşehir during the instrumental period. In 1911, a strong earthquake (I:VIII) caused various damage in Bolvadin and Çay; a geothermal spring near the Heybeli baths started to flow after this earthquake (Pınar and Lahn, 1952; Özer, 2006; Başaran and Gökgöz, 2016). Some moderate earthquakes occurred in Bolvadin between 1914 and 1915 (Ergin et al., 1967; Özer, 2006). During the instrumental period, a series of strong earthquakes with magnitudes between 5.7 and 6.3 caused seismic migration northwestward towards the Sultandağı fault. The sequence started with the 26 September 1921 Argıthanı earthquake (Ms: 5.9, Table 1). Then continued with the Akşehir earthquake on 21 February 1946 (Ms: 5.7, Table 1), and Sultandağı earthquake on 15 December 2000 (Mw: 6.0, Table 1) (Demirtaş et al., 2002; Emre et al., 2003). The latest one occurred on 3 February 2002 (Mw: 6.3). The epicenters are located in the middle part of the graben, south of Bolvadin city. On the other hand, the seismicity of Bolvadin is sparse and the majority of earthquakes have been small-moderate intensity during the instrumental period. Recently, 20 focal mechanism solutions for some earthquakes (Mw: 3.3–6.3) indicating the existence of an extensional tectonic regime were reported along the AAG (Erdik et al., 2002; Tan et al., 2008; Kalafat and Görgün, 2017; Tiryakioğlu et al., 2018) (Figure 2).

3. The Bolvadin Fault

The Bolvadin Fault is a NE–SW-trending structure with prevailing dip-slip kinematics affecting the northern boundary of the AAG. It is located at the north of the most

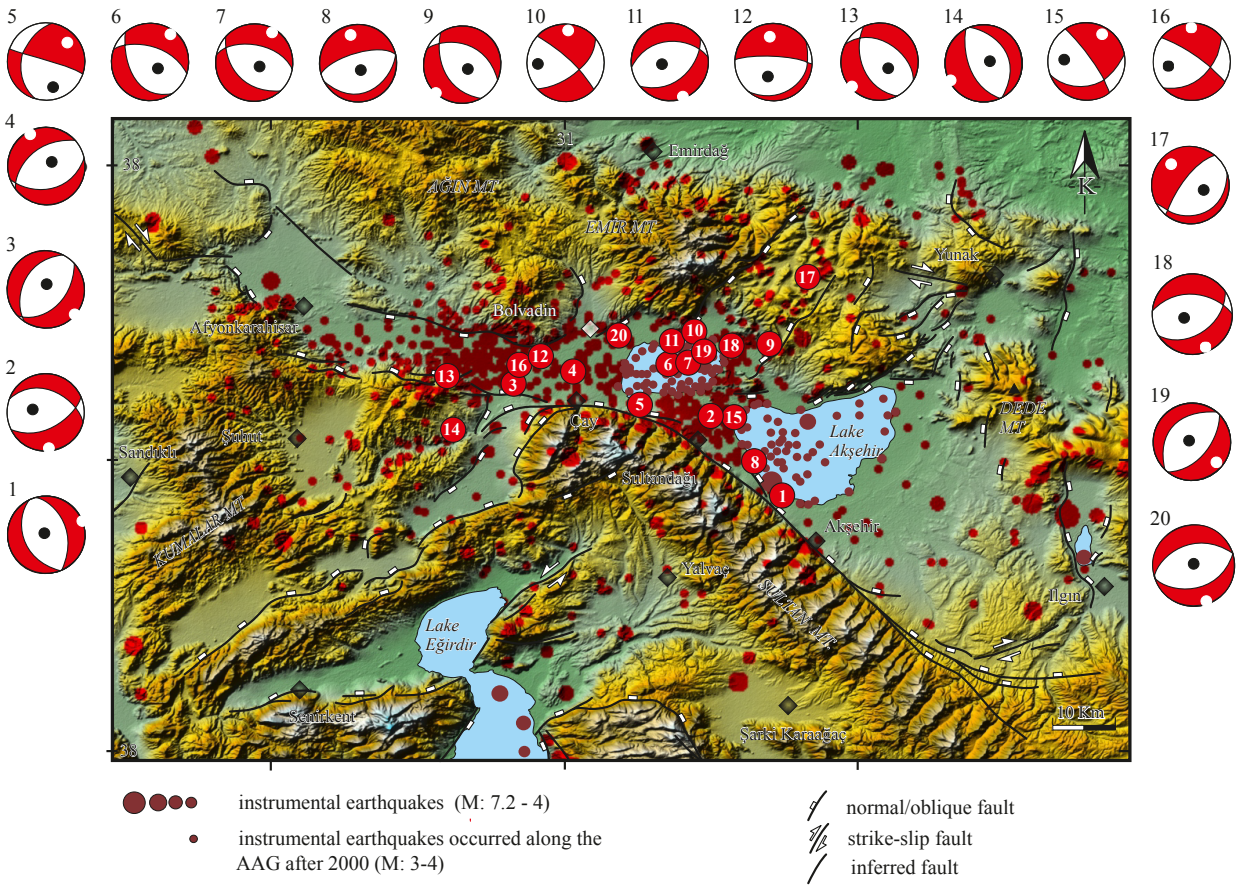


Figure 2. Seismotectonic map of the Afyon–Akşehir Graben (faults are taken from Emre et al., 2011; results of the focal mechanism solutions of earthquakes that occurred in the AAG taken from Erdik et al. (2002), Tan et al. (2008), KOERI (2019), Taymaz and Tan. (2001), Kalafat and Görgün (2017), and Tiryakioğlu et al. (2018). Earthquake data (M: 3–4) are taken from KOERI (2019). Please see Tiryakioğlu et al. (2018) for details about the numbered earthquakes.

recent surface ruptures generated by the 3 February 2002 Çay earthquakes (Mw: 6.3 and 6.0, Figure 3) along the Sultandağı fault which is also known as the northeastern outer border of the Isparta Angle. Geologic mapping indicates that it has a southeast dip direction extending approximately 16 km between Bolvadin city center to the southwest and Erikliburnu Hill to the northeast with the approximate width of the fault zone about 2 km. The Bolvadin Fault consists of several parallel/subparallel fault segments. Three lithostratigraphic units separated by regional unconformities were mapped along the Bolvadin Fault. These are (i) pre-Neogene metamorphic basement

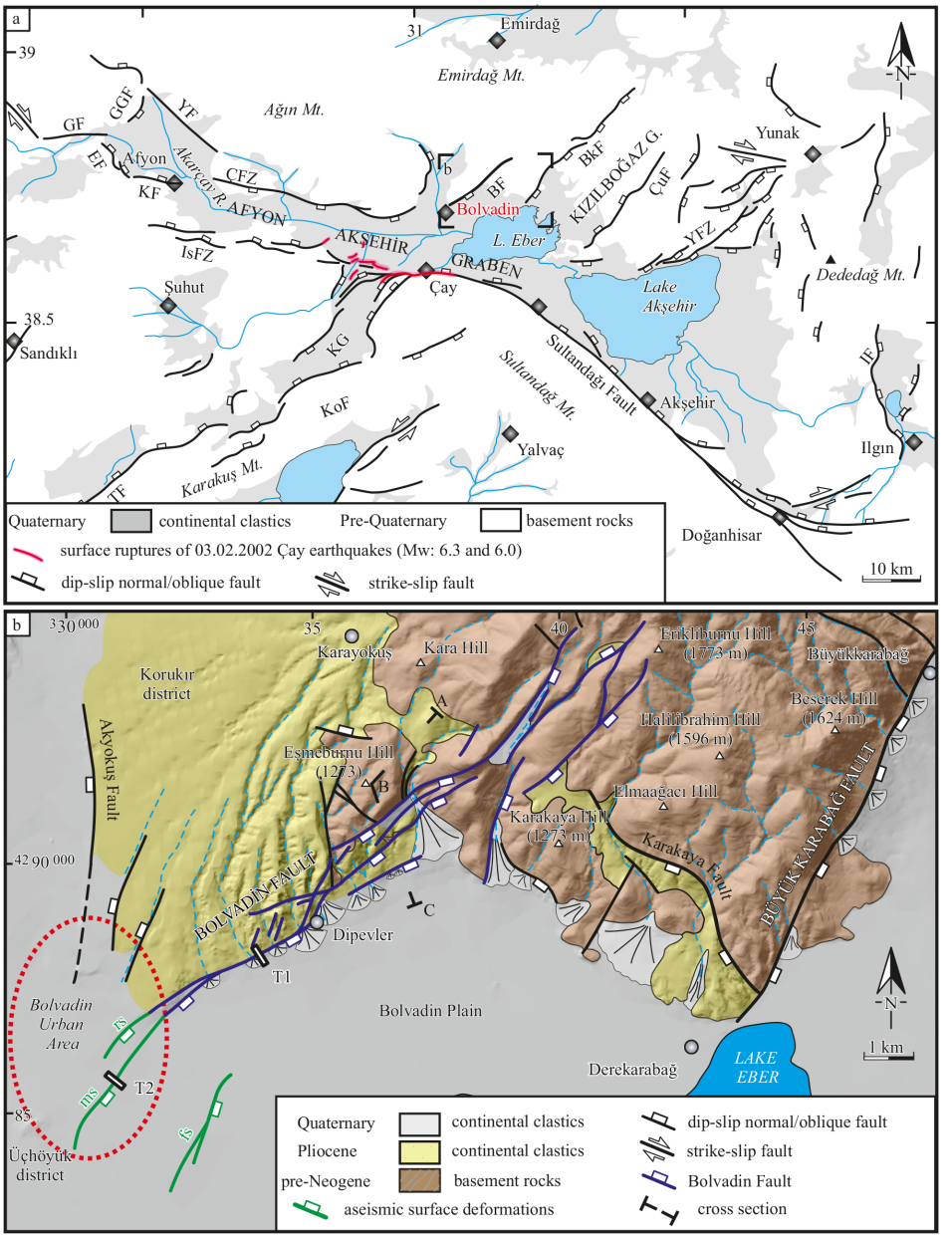


Figure 3. a) The active fault map of the AAG (issued from Emre et al., 2011) Abbreviations: KG: Karamık Graben; GF: Gecek Fault; GGF: Gazlıgöl Fault, EF: Erkmen Fault; KF: Karahisar Fault; ÇFZ: Çobanlar Fault Zone; IsFZ: Işıklar Fault Zone; YFZ: Yunak Fault Zone; IF: Ilgın Fault; BF: Bolvadin Fault; BkF: Büyük Karabağ Fault; ÇuF; Çukurcak Fault;YF: Yarıkkaya Fault; KoF: Kocbeyli Fault; TF: Tatarlı Fault. b) Geological map of the Bolvadin district. Abbreviations: rs: rear splay, ms: middle splay, and fs: front splay; T1: trench 1, T2: trench 2.

rocks of Afyon Zone, primarily consisting of marble and schist, (ii) Pliocene continental sediments alternating within a volcano-sedimentary sequence, and (iii) Holocene modern graben fill consisting of alluvial fan, fluvial and colluvial deposits (Figure 3). At the northeastern end of the Bolvadin Fault, the NW–SE-striking Karakaya Fault represents a breached relay ramp area between the NE–SW-striking Büyük Karabağ and Bolvadin Faults. Pliocene sediments and pre-Neogene basement rocks are juxtaposed along 6 km in the linkage area.

The Bolvadin Fault cuts and deforms the pre-Neogene basement rocks, which consist of extensive marble rocks exposed on the northeastern part of the fault where the fault scarp is morphologically prominent. Along these steep topographic scarps, well preserved slip surfaces and fault-related structures such as fault striations, grooves, corrugations, fault breccias, and weathering bands can be observed (Figure 4). Well-exposed outcrops of the Bolvadin Fault document a strike between N50 and 70°E with an average 55–65°dip and pitches of slip lines average 75–85°; thus, showing the dip-slip normal character of the Bolvadin Fault. An approximate NW–SE extensional stress regime on NE–SW-trending dip-slip normal faulting is also compatible with the geomorphologic markers such as the formation of alluvial fans and triangular facets on the linear mountain front. The linear and steep topographic fault scarps on the field observations show that the corrugated polished slip surface of the Bolvadin Fault separates young colluvial fans from basement rocks. On the exposed fault plane, we identified differently weathered bands which are parallel to the scarp base and laterally continuous. The upper band is less polished within small karstic fissures and unclear slip lines. However, the 15 cm-high lower band shows that it is a well-preserved and polished fault, related to structures such as corrugations, striations, gutters, and tool tracks (Figure 4).

Along the middle part of the fault near Dipevler, numerous quasiparallel SE-dipping normal fault fragments form a step-like geometry (Figure 5). The overall width of the fault zone is about 1 km in this section. Pre-Neogene carbonates from the bedrock and unconformably overlying Pliocene clastics are cut and deformed by these structures causing the formation of alluvial/colluvial deposits on the hanging wall. According to geological mapping and correlating the basal unconformity of Pliocene clastics on both sides of the Bolvadin Fault, the maximum vertical displacement is about 500 m (Figure 5).

West of the Bolvadin Fault, there is a set of minor N–S, antithetic (i.e. west-dipping) normal faults about 4 km-long (Akyokuş Fault) delimiting the Pliocene unit, and this may have formerly been a sort of horst. The geometrical relationship between the two faults towards the south is not clear because the Akyokuş Fault is buried under modern graben fill (Figure 3).

3.1. Aseismic surface deformations

Some settlements, which are established on active faults in Western Anatolia experienced aseismic surface displacement characterised by well-defined linear scarps in the last 10–20 years (Gürsoy et.al., 1997; Demirtaş et al., 2008; Koca et al., 2011; Özalp et al., 2011; Özkaymak et al., 2014; 2017). In such settlement areas, this kind of surface deformation also causes serious damage to urban buildings and infrastructure and has considerable economic impact. Prominent examples of such deformations that formed without a destructive earthquake failure observed in the Bolvadin settlement area are shown in Figure 6. During the field studies we mapped these linear surface deformations at a scale of 1/5000, forming three distinct splays along the southwestern part of the fault. The rear primary splay (rs), a 1.5 km-long northwestward arched linear deformation, trends N70°E for some distance northeast of Kale, around the old cemetery extending parallel to the main road between Bolvadin and Dipevler. Around the new cemetery it bends to N30°E direction (Figure 4). The middle section (ms) of the surface deformation is about 3 km long and quite linear (N30°E), lying between Akçan park in the southwest and Kale in the northeast. Rs, ms, and the master fault of Bolvadin merge in Kale. The front primary splay (fs) is also 3 km long and roughly parallel to the ms but located in approximately 2 km southeast of it. Vertical displacements up to 70 cm based on precise levelling were also obtained by Tiryakioğlu et al. (2019) along the progressive surface deformation. According to precise levelling surveys across the middle splay, a vertical surface displacement rate of 40 mm/year was detected in the years 2016-2018, while the average throw rate along these three splays is 85 mm/year (Tiryakioğlu et al., 2019).

4. Palaeoseismology

Two trench sites were selected as a result of geologic and geomorphologic surface mapping studies on the Bolvadin Fault. These are the first example of palaeoseismological investigations across creeping faults in Turkey. The first trench was excavated on prominent scarps of the Bolvadin master fault between the settlement area of Bolvadin and Dipevler where the fault is linear and aseismic deformation is not observed. The Bolvadin Fault represents the structural contact between Pliocene sediments and Holocene clastic deposits of fluvial and colluvial origin. The second trench was excavated across the aseismic surface deformation (on the middle splay) in the settlement area of Bolvadin (Figure 3) in order to understand (1) underground geometry of these deformations, (2) whether the active surface deformations followed a preexisting fault, and (3) palaeoseismic history if they follow the Bolvadin Fault. Both trenches were excavated perpendicular to the morphological scarps. The microstratigraphy was determined by mapping the trench

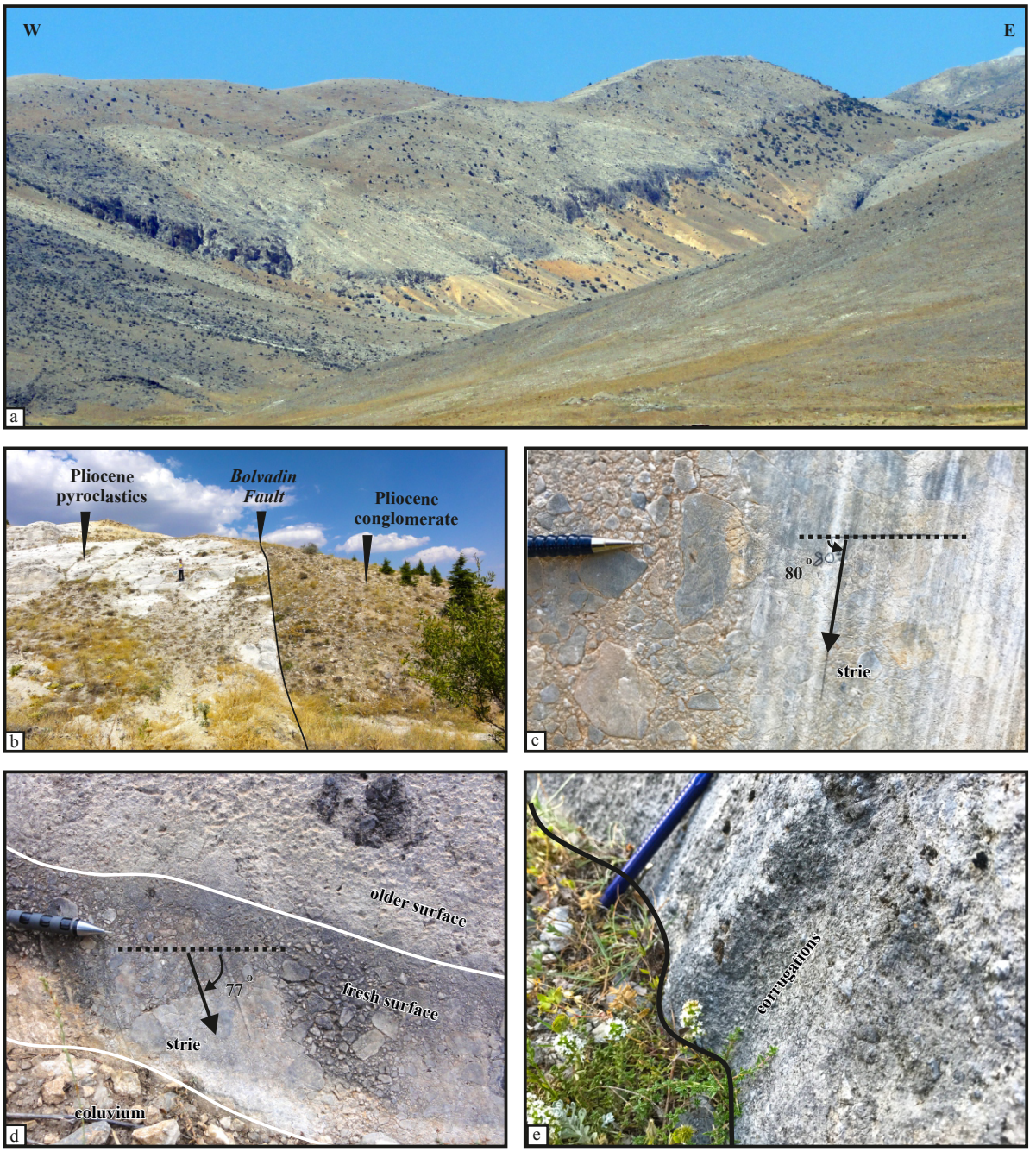


Figure 4. a) Field view from the northeastern and b) middle parts of the Bolvadin Fault, c-d-e) close-up view of the fault plane showing slip surface features, which indicate the normal character of the fault.

walls and based on C14 dating of the lithostratigraphic units. Radiocarbon ages were calibrated to calendar years using the software OxCal 4.3.2 (Bronk Ramsey, 2017) and based on atmospheric data from Reimer et al. (2013). Dating analyses were carried out in the laboratories of Beta Analytic Inc. (Miami, FL, USA).

4.1. Bolvadin - 1 trench (T1),

Trench-1 (T1) is oriented N20°W, 25 m long and up to 3 m deep and wide. Both trench walls were logged at 1:20 scale and show evidence of a dip-slip normal faulting. Both walls contained 8 lithologic units, stratigraphically the first five are defined as fluvial succession with well-stratified beds.

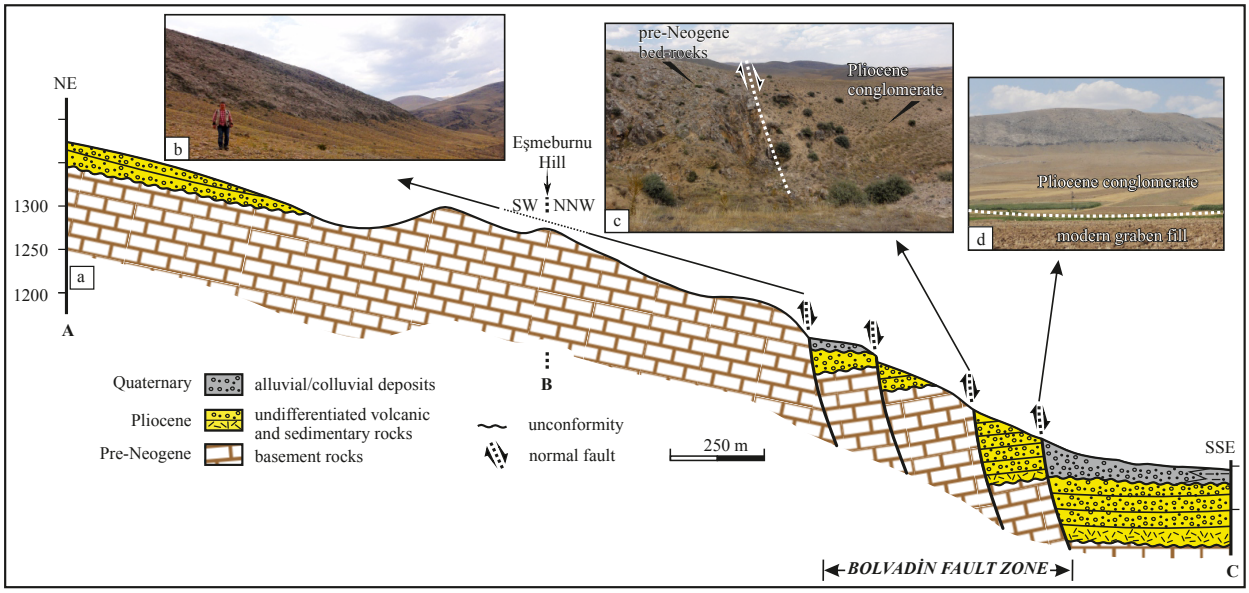


Figure 5. a) Geologic cross-sections showing step-like fault morphology, b-c-d) Field views of parallel faults.



Figure 6. Field photographs showing the vertical displacement along the a) ms, b) fs, and c) rs (Özkaymak et al., 2017).

Since the succession dips slightly towards the northeast by a few degrees, the SW wall also shows the uppermost parts of the section. The basement of the fluvial series (unit 1) consists of alternating light greyish cream gravelly muddy clay and brown clayey mud exposed on the southeast side of the trench walls. Unit 1 is overlain by a light yellowish brown clayey sandy mud (Unit 2). The overlying unit 3 starts with a sandy matrix rich in subrounded to rounded gravels and has an erosive base, while the unit grades upwards to cross-bedded gravelly coarse-grained sand. Unit 4 consist of grey clayey sandy mud. The base levels of unit 5 start with light green cross-bedded gravelly sands and fine upwards to light yellowish brown fine grained sandy clayey mud. The uppermost levels of unit 5 contain dark grey well-rounded, normally graded, commonly matrix-supported fine gravels. The fluvial succession is covered by unit 6 showing characteristics of colluvial wedge facies and is composed of light brown gravelly sandy mud. The V-shaped unit 7 is interpreted as crack fills consisting of brown gravelly sandy mud, which is mainly derived from unit 6. Unit 8 represents the recent soil cover, consisting of dark brown organic rich mud (Figure 7).

Based on the stratigraphic, sedimentologic, and structural analysis of the trench walls, at least two events were identified in Bolvadin 1 trench. During the first event, the entire fluvial succession observed in the trenches is cut and deformed by many antithetic and synthetic normal faults covered by the colluvial deposits of unit 6. Organic bulk sediment (sample B1C1, Table 2) from deformed unit 2 yielded a radiocarbon age of 2570 ± 30 14C cal yr BP. The radiocarbon samples (B1C3 and B1C6, Table 2) collected from the colluvial deposits (unit 6) covering the first event gave a calibrated age between 490 and 470 ± 30 (BP). Colluvial deposits from unit 6 are clearly cut by the younger fault splays causing the formation of crack opening in different parts of the trench wall. This is related to the second event. Thus, the youngest event occurred after deposition of unit 6 and before deposition of unit 7, which yielded radiocarbon ages of 380 and 310 ± 30 (BP) (samples B1C2 and B1C5, Table 2).

Along the average N75°E-trending and 17 m wide deformation zone, measured vertical displacements range between roughly 1.5 and 2.1 m in both trench walls (Table 3). By correlating the top of unit 2 (2570 ± 30 years, BP) on either side of the fault, we measured a vertical offset of 161–165 cm on NE and SW walls, respectively. Thus, the vertical late Holocene slip rate determined from cumulative displacement across the fault is ca 0.63 mm/year (Table 3).

4.2. Bolvadin - 2 trench (T2),

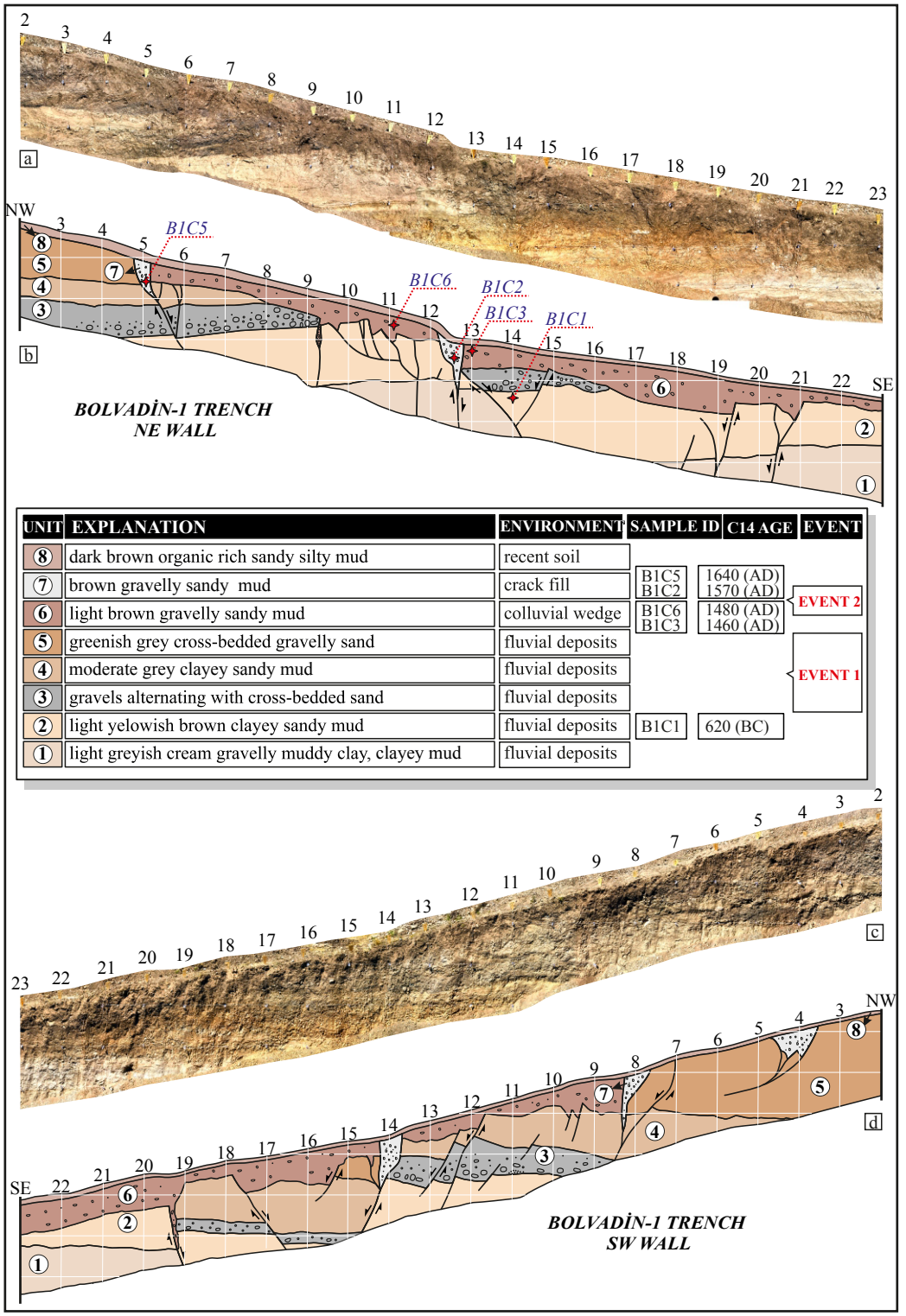
Due to the active surface displacement (middle part of the ms) along the fault at this location, geomorphic scarp expression is very clear. Thus, the N50°W oriented trench 2 was excavated across the N55E-trending deformation trace. It was nearly 3 m wide, about 10 m long and 4 m deep. Both trench walls were logged at a 1:20 scale. Trench walls contain seven stratigraphic units consisting of generally horizontally layered fluvial deposits. The lowest unit consists of light brownish clayey mud including light yellowish beige gravelly sand interbeds. Unit 2 is interpreted as the crack fills comprising brownish grey gravelly muddy sand. Overlying unit 3 is composed of light bluish grey cross-bedded gravelly sands. Well-rounded, well-sorted, and polygenic gravels are mostly derived from schist, marble, and andesites. The texture is mainly sandy matrix-supported. The base of the unit is locally erosional associated with the emplacement on the underlying units 1 and 2. A light brown palaeosol unit consisting of organic rich silty mud (unit 4) covers unit 3 with a sharp base.

The overlying unit 5 starts with light brown gravelly clayey mud including wedge-shaped sandy gravels. Towards the upper parts, unit 5 includes immature debris gravel in a muddy sandy matrix. Unit 6 is recent soil consisting of dark brownish organic rich silty mud. The uppermost unit (unit 7) is colluvium comprising of light grey gravelly sand, mostly derived from the unit 5. A wide crack that was opening as a result of aseismic surface deformation since 2012 was still being filled with that colluvium (unit 7) which also covers the recent soil on the southeastern dropped block (Figures 8 and 9).

Trench studies at this site suggest that a surface rupture event occurred before the aseismic surface deformation process. This event deforming unit 1 also caused the surface cracks to be filled by unit 2 which is overlain by fluvial deposits of unit 3. Thus, the radiocarbon sample B2C2 collected from the upper part of unit 1 yielded a radiocarbon age of 1650 ±30 (BP) representing the lower boundary of the event. Unfortunately, we were not able to find sufficient samples to date the upper boundary of units 2 and 3. Furthermore the radiocarbon sample of charcoal collected from unit 4 gave an unsuitable result, most probably it was allochthonous. Hence, the upper boundary of the event is defined according to the radiocarbon age of unit 5 (sample B2C5, Table 2) which yielded an age of 370 ± 30 (BP).

5. Discussion and conclusions

In this study, detailed geological mapping and palaeoseismological investigations were performed along the Bolvadin Fault documenting aseismic surface deformations following previous linear morphogenic earthquakes (Caputo, 2005). The origin and formation mechanism of these surface deformations that have been formed in the last 10–20 years in western Anatolia are still under debate. However, there is a consensus about the role of groundwater withdrawal from unconsolidated sediments due to the effect of groundwater pumping by human activities and natural drought are important



UNIT	EXPLANATION	ENVIRONMENT	SAMPLE ID	C14 AGE	EVENT
8	dark brown organic rich sandy silty mud	recent soil			
7	brown gravelly sandy mud	crack fill	B1C5 B1C2	1640 (AD) 1570 (AD)	EVENT 2
6	light brown gravelly sandy mud	colluvial wedge	B1C6 B1C3	1480 (AD) 1460 (AD)	
5	greenish grey cross-bedded gravelly sand	fluvial deposits			EVENT 1
4	moderate grey clayey sandy mud	fluvial deposits			
3	gravels alternating with cross-bedded sand	fluvial deposits			
2	light yelowish brown clayey sandy mud	fluvial deposits	B1C1	620 (BC)	
1	light greyish cream gravelly muddy clay, clayey mud	fluvial deposits			

Figure 7. (a) Oblique photomosaic and (b) log of NE wall of trench-1; (c) Oblique photomosaic and (d) log of SW wall of trench-1.

Table 2. Samples collected from trenches and the results of radiocarbon dating.

Trench/unit no	Sample number	Lab. ID no	Material type	Radiocarbon age (BP) (95.4 %)	Two sigma range
1/6	B1C3	Beta - 491747	Organic sediment	490 ± 30	1404–1450 (AD)
1/2	B1C1	Beta - 491748	Organic sediment	2570 ± 30	809–748 (BC)
1/7	B1C2	Beta - 491749	Organic sediment	380 ± 30	1445–1632 (AD)
1/7	B1C5	Beta - 491751	Organic sediment	310 ± 30	1485–1650 (AD)
1/6	B1C6	Beta - 491752	Organic sediment	470 ± 30	1410–1457 (AD)
2/5	B2C5	Beta - 491745	Charcoal	370 ±30	1446–1634 (AD)
2/1	B2C2	Beta - 491746	Potsherd Residue	1650 ±30	330–433 (AD)

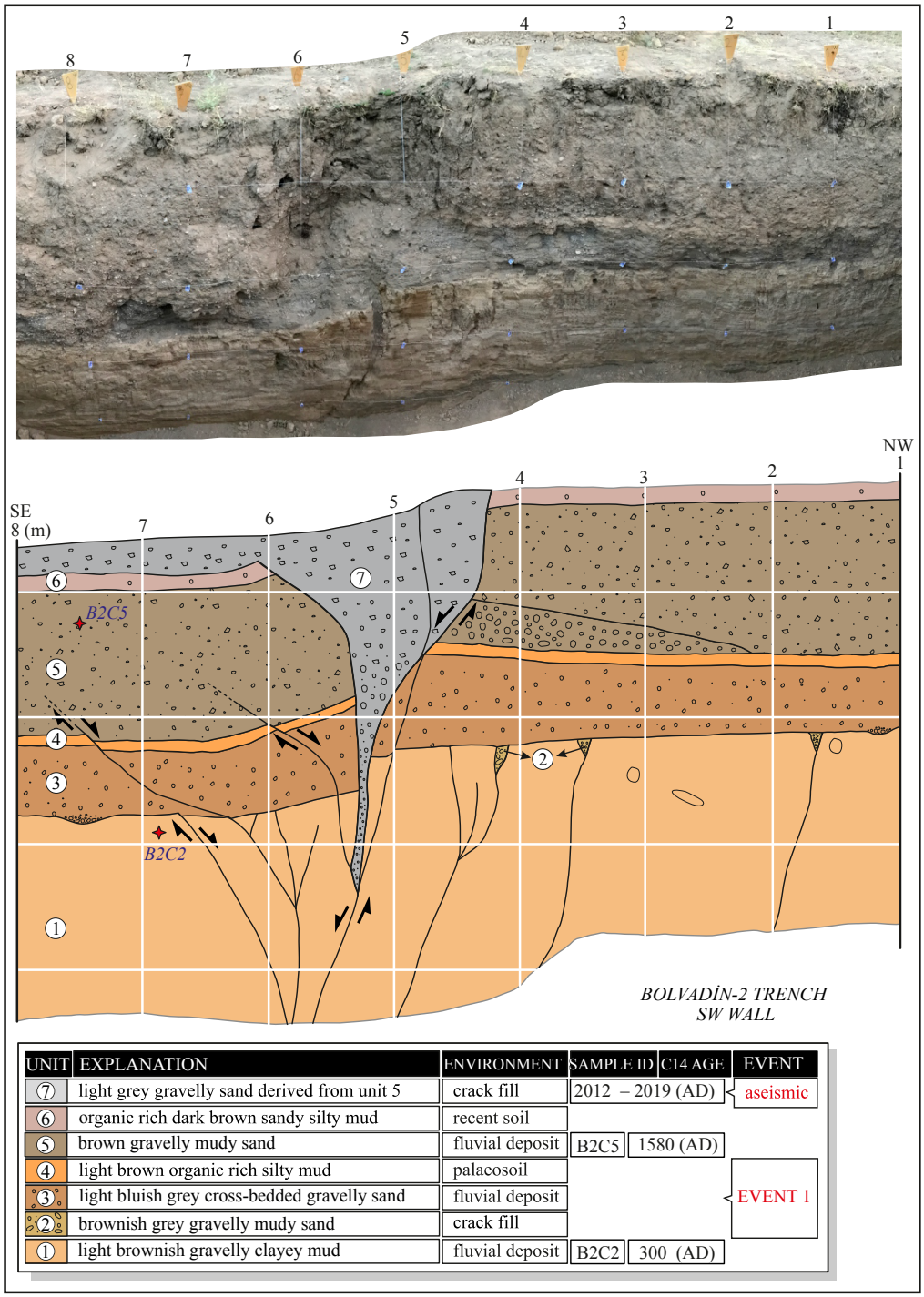
Table 3. Vertical displacement values measured in trench 1 and obtained palaeoseismologic slip rate values.

Lithology	Age (BP)	Vertical displacement		Slip rate (mm/year)
		SW Wall (cm)	NE Wall (cm)	
Unit 5	-	190	-	-
Unit 4	-	184	-	-
Unit 3	-	211	164	-
Unit 2	2570 ± 30	165	161	0.63-0.64
Unit 1	-	-	202	-

agents for this kind of aseismic surface failure (Gürsoy et al., 1997; Demirtaş et al., 2008; Koca et al., 2011; Özalp et al., 2011; Özkaymak et al., 2014, 2017, 2018; Demirtaş and Tepeuğur., 2017). According to Gürsoy et al. (1997) microseismic activities are the crucial reason, while Demirtaş and Tepeuğur (2017) and İmamoğlu et al. (2019) claim that the only reason is groundwater withdrawal. Koca et al. (2011) and Özkaymak et al. (2014; 2017; 2018) suggest that in addition to compaction of sediments due to the withdrawal of underground fluids, microseismic activity and tectonic creep can also play some role. Indeed, considering the viscoelastic rheology of rocks (Melosh, 1980; Wang, 1995), the 2002 Çay earthquakes (Mw: 6.3–6.0) clearly increased the accumulation of elastic strain energy on the northern border of the graben, where Bolvadin stands, and caused some additional tectonic loading. We suggest that postseismic creep and high microseismic activity are probably accompanied by compaction of alluvial/fluvial sediments induced by the fall in groundwater level that dropped 22 m in Bolvadin city center since 2002. As we documented earlier, after the 2002 Çay earthquakes, some progressive aseismic surface deformations began to develop as three prominent splays in Bolvadin city center (southwestern part of the Bolvadin Fault) whose length is up to 4 km with vertical displacements up to 70 cm. According to the precision level measurements performed by Tiryakioğlu et al. (2019), the average rate of vertical displacement along these three splays is 85 mm/year. The deformation rate is compatible with the general values (between 6 and 10 cm/year) obtained from similar deformation regions in western Anatolia and USA (Holzer, 1984; Koca et al., 2011; Poyraz et al. 2015; Özkaymak et al., 2017).

Detailed geological mapping studies clearly indicate that maximum vertical displacement between the basal unconformity of Pliocene clastics (5 Ma) on the footwall and the hanging wall is estimated as approximately 500 m in the middle of the fault where aseismic surface deformation is not observed (Figure 6). This yields a mean geological slip rate of about 0.1 mm/year since the Pliocene for the Bolvadin Fault. This slip rate value best fits with the rates calculated for dip-slip normal faults in western Anatolia, Greece, and Italy (Caputo, 1995; Caputo et al., 2004; Pavlides and Caputo, 2004; Papanikolaou et al., 2005; Özkaymak et al., 2011; Özkaymak, 2015; Tsodoulos et al., 2016; Özalp et al., 2018).

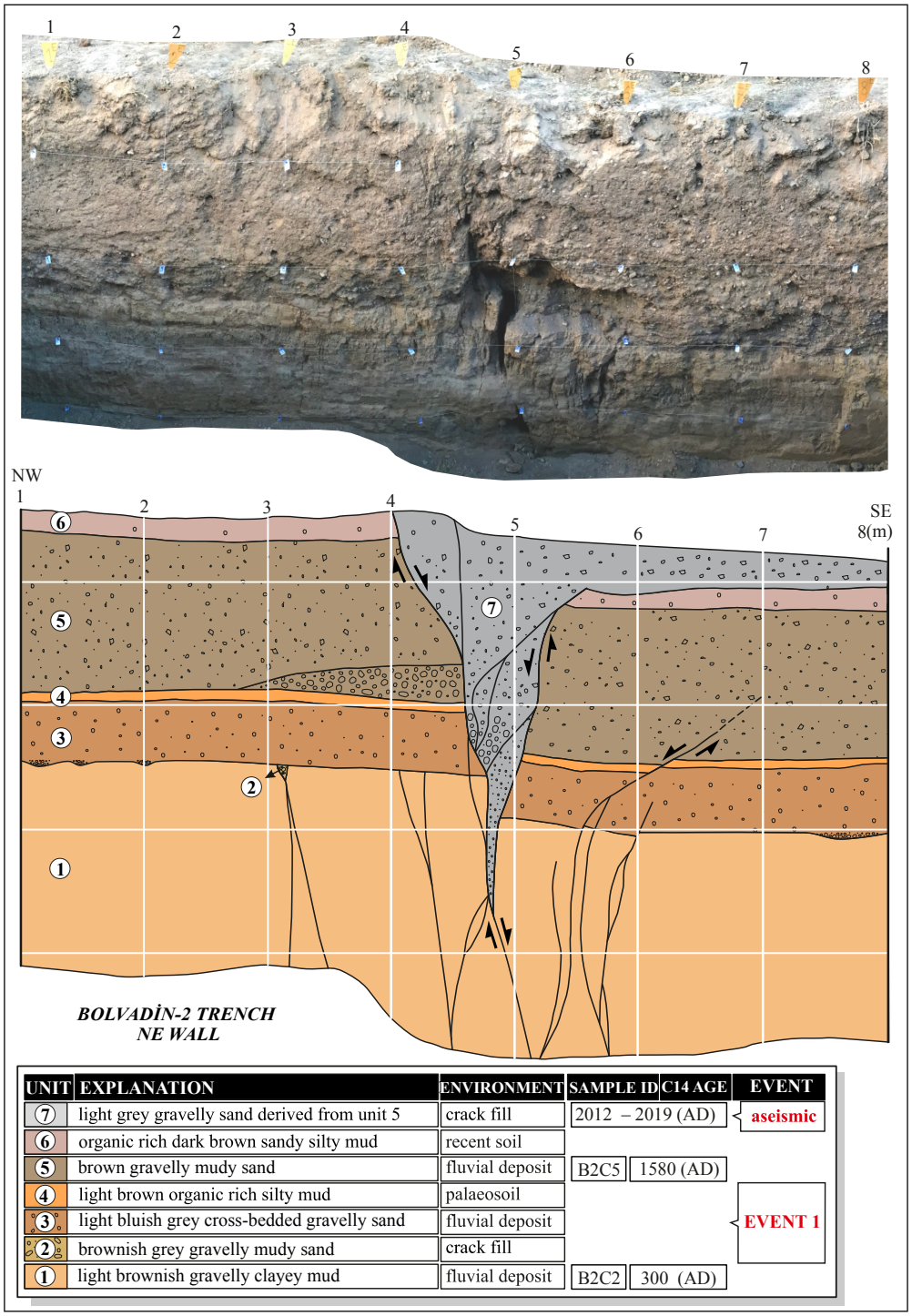
We can also estimate the magnitude of the slip rate during late Holocene according to palaeoseismological results. By correlating stratigraphic unit 2 in trench 1 with radiocarbon age of 2570 ± 30 years, a vertical offset of 161–165 cm could be measured in the trench walls. Thus, the late Holocene throw-rate, which was determined



UNIT	EXPLANATION	ENVIRONMENT	SAMPLE ID	C14 AGE	EVENT
⑦	light grey gravelly sand derived from unit 5	crack fill	2012 – 2019 (AD)		aseismic
⑥	organic rich dark brown sandy silty mud	recent soil			
⑤	brown gravelly mudy sand	fluvial deposit	B2C5	1580 (AD)	
④	light brown organic rich silty mud	palaeosoil			EVENT 1
③	light bluish grey cross-bedded gravelly sand	fluvial deposit			
②	brownish grey gravelly mudy sand	crack fill			
①	light brownish gravelly clayey mud	fluvial deposit	B2C2	300 (AD)	

Figure 8. Photomosaic and log of SW wall of trench-2.

from cumulative displacement across the fault, is about 0.63–0.64 mm/year (Table 3). This estimation cannot include the amount of aseismic throw because trench 1 was excavated on the master fault around Dipevler where aseismic surface deformation is not observed. The Bolvadin Fault is defined as a 7 km-long normal fault on the active fault map of Turkey by Emre et al. (2011). Hence, the earthquake production capacity of the fault is calculated as a moment magnitude of 5.98 (Emre et al., 2018). However, our geologic mapping and trench



UNIT	EXPLANATION	ENVIRONMENT	SAMPLE ID	C14 AGE	EVENT
7	light grey gravelly sand derived from unit 5	crack fill	2012 – 2019 (AD)		aseismic
6	organic rich dark brown sandy silty mud	recent soil			
5	brown gravelly mudy sand	fluvial deposit	B2C5	1580 (AD)	
4	light brown organic rich silty mud	palaeosoil			
3	light bluish grey cross-bedded gravelly sand	fluvial deposit			EVENT 1
2	brownish grey gravelly mudy sand	crack fill			
1	light brownish gravelly clayey mud	fluvial deposit	B2C2	300 (AD)	

Figure 9. Photomosaic and log of NE wall of trench-2.

studies indicate that it extends approximately 16 km from Bolvadin city center to the southwest and Erikliburnu Hill to the northeast (Figure 3b). Thus, based on empirical relationships (Wells and Coppersmith 1994; Pavlides and Caputo 2004), it could generate an earthquake with a moment magnitude of 6.48. This magnitude on crustal faults can certainly produce surface ruptures and our trench-based palaeoseismological studies confirm that the Bolvadin Fault generated at least two linear morphogenic earthquakes during the last two millennia.

It was observed in trench 1 that the first event occurred between 620 (BC) and 1460 (AD) and the second event occurred between 1480 (AD) and 1570 (AD) (Figure 10). In trench 2, the observed event took place between 300 AD and 1580 AD. Besides this, burial palaeosol (unit 4) overlying the first event in trench 2 also indicates that one more event may have occurred after the penultimate event and before 1580 (AD) in trench 2. This possibility may correlate with the second event in trench 1. On the other hand, the formation of NW-dipping antithetic faults deforming unit 4 (trench 2, Figures 8 and 9) in the hanging wall is probably associated with aseismic surface deformation. The first event which is observed in both trenches can be associated with the 530 (AD) earthquake,

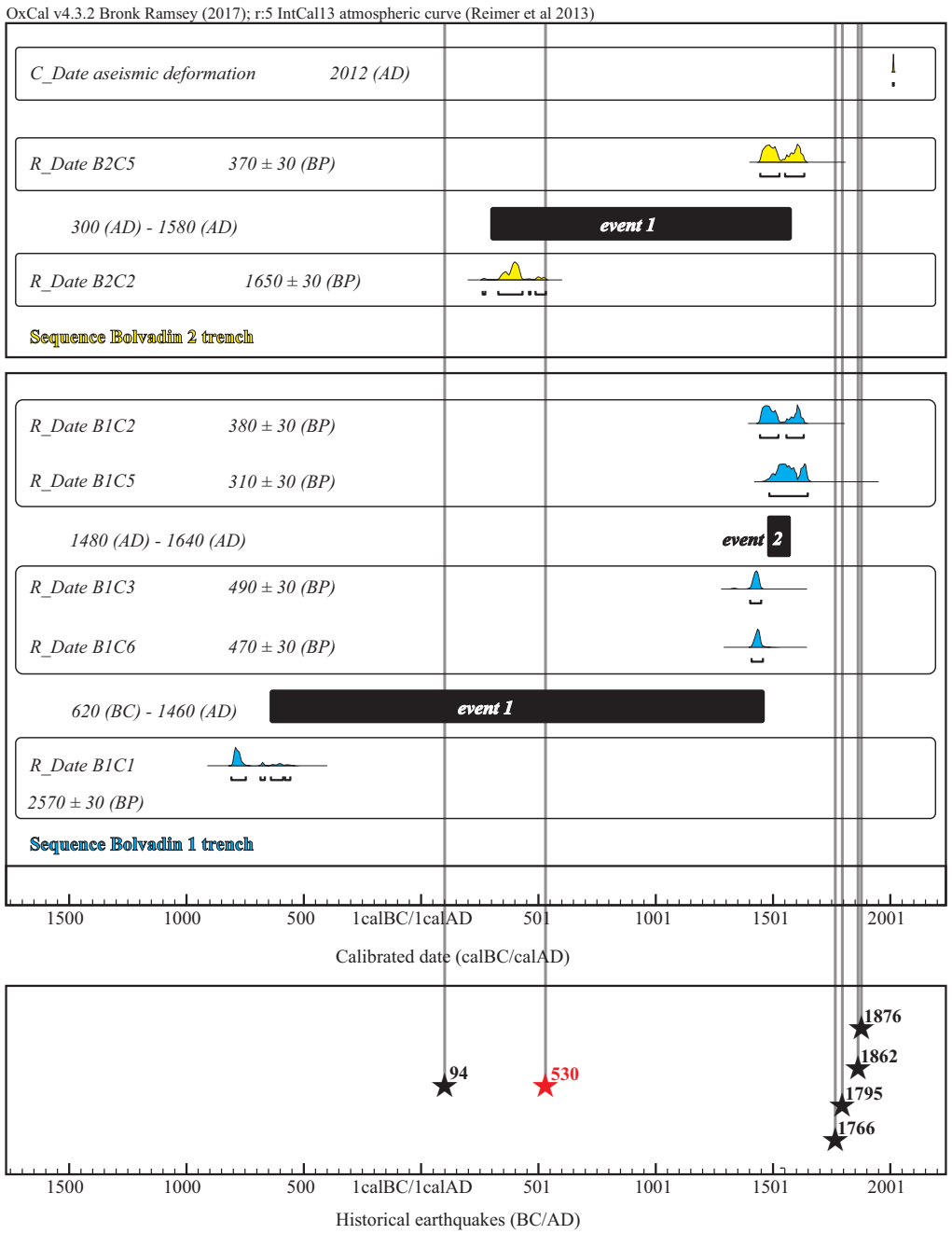


Figure 10. Probability distribution of calibrated C14 ages and related probability density functions according to OxCal v.4.3.2 (Bronk Ramsey, 2017; Reimer et al., 2013).

which is stated to have destroyed Bolvadin city center in historical records (Ambraseys, 2009). The second event probably occurred in 1525 ± 45, though there is no record of any large earthquake in AAG and the nearby area in the historical record. On the other hand, the estimated recurrence interval for surface rupture earthquakes is 995 ± 45 years. This result best fits with a recurrence interval estimate of 910 ± 40 years on the Erdoğmuş Fault (Gediz) in the ASFS by Gürboğa et al. (2013). The time since the last morphogenic (M > 6) earthquake for the Bolvadin Fault is 494 ± 45 years.

If we compare the geologic and palaeoseismologic slip rates (0.1 mm/year for Pliocene; 0.64 mm/year for late Holocene, respectively) for the Bolvadin Fault, they all agree it has moderate activity (0.1 < slip rate < 1 mm/year) according to Bonilla's (1982) classification. This result also best fits with the calculated recurrence interval of about 1 ka for the Bolvadin Fault considering the potential fault displacement prediction is between 10 cm and 1 m for every 1 ka with a maximum magnitude of Mw 6.48.

The presence of scarp base-parallel weathered bands on exposed fault planes suggests that scarp formation and fault plane exposure resulted from repeated fault activation (e.g. Caputo, 1993, 2005; Stewart 1996; Giaccio et al., 2002). This interpretation is based on the assumption that the degree of weathering is a function of the exposure time of a rock surface. A possible method for dating such bands on exposed carbonate fault scarps is based on cosmogenic ^{36}Cl measurement techniques (e.g., Akçar et al., 2012; Mozafari et al., 2019) that could be applied in future studies. Besides this, along the aseismic surface creep of the Bolvadin Fault, underground data using drilling and seismic reflection methods should be generated for further studies in order to determine the compaction of sediments, calculate the possible tectonic creep rate, and analyse the underground geometry.

Acknowledgments

This research was supported by the Scientific Research Council of Turkey (TÜBİTAK) (project number: 115Y246) and Afyon Kocatepe University Research Foundation (project number: AKÜ-BAP 16.KARİYER.167). We are grateful to Ahmet Cançeker and Arda Özkaymak for their help during field studies and Elif Yiğit for English language editing. The final version of the paper was edited by Skaian Gates English editing service.

References

Akçar N, Tikhomirov D, Özkaymak Ç, Alfimov V, Ivy-Ochs S et al. (2012). 36Cl Exposure Dating of Palaeoearthquakes in the Eastern Mediterranean: First Results from the Western Anatolian Extensional Province, Manisa Fault Zone, Turkey. Geological Society of America Bulletin 124 (11/12): 1724-1735.

Aktug B, Nocquet JM, Cingoz A, Parsons B, Erkan Y et al. (2009). Deformation of western Turkey from a combination of permanent and campaign GPS data: Limits to block-like behavior. Journal of Geophysical Research 114: B10404.

Akyüz S, Uçarkuş G, Şatır D, Dikbaş A, Kozacı Ö (2006). 3 Şubat 2002 Çay depreminde meydana gelen yüzey kırığı üzerinde palaeosismolojik araştırmalar. Yerbilimleri 27(1): 41-52 (in Turkish).

Ambraseys NN (1988). Engineering Seismology. Earthquake Engineering and Structural Dynamics 17: 1-105.

Ambraseys NN, Jackson JA (1998). Faulting associated with historical and recent earthquakes in the Eastern mediterranean region. Geophysical Journal International 133: 390-406.

Ambraseys N (2009). Earthquakes in the Mediterranean and Middle East: a multidisciplinary study of seismicity up to 1900. New York, United States of America: Cambridge University Press.

Başaran C, Gökgöz A (2016). Hydrochemical and isotopic properties of Heybeli geothermal area Afyon Turkey. Arabian Journal of Geosciences 9 (11): 586.

Bonilla MG (1982). Evaluation of Potential Surface Faulting and Other Tectonic Deformation. USGS Open-File Report 82-732 Version 1.1. [online]. Website http://pubs.usgs.gov/of/1982/of82-732/ [accessed 13 May 2019].

Bronk Ramsey C (2017). Methods for summarizing radiocarbon datasets. Radiocarbon 59 (6): 1809-1833.

Burtford RO, Harsh PW (1980). Slip on the San Andreas fault in central California from alignment array surveys. Bulletin of the Seismological Society of America 70: 1223-1261.

Caputo R. (1993). Morphogenic earthquakes: a proposal. Bulletin of the Inqua Neotectonics Commission 16: 24.

Caputo R. (1995). Inference of a seismic gap from geological data: Thessaly (Central Greece) as a case study. Annals of Geophysics 38 (1): 1-19.

Caputo R. (2005). Ground effects of large morphogenic earthquakes. Journal of Geodynamics 40 (2-3): 113-118.

Caputo R, Helly B, Pavlides S, Papadopoulos G (2004). Palaeoseismological investigation of the Tyrnavos Fault (Thessaly, Central Greece). Tectonophysics 394: 1-20.

Çakır Z, AM Akoğlu, S Belabbes, S Ergintav, Meghraoui M (2005). Creeping along the Ismetpasa section of the North Anatolian fault (Western Turkey): Rate and extent from InSAR. Earth and Planetary Science Letters 238: 225-234.

Demirtaş R, Iravul Y, Yaman M. (2002). 3 Şubat 2002 Eber ve Çay depremleri ön raporu. Jeoloji Mühendisliği Haber Bülteni 2002/(1-2): 58-63 (in Turkish).

Demirtaş R, Ercan S, Demir B, Aktan M (2008). Ege çöküntü bölgesi'nde alüvyal havzalarda son 20 yılda oluşmuş yüzey deformasyonlarının oluşum mekanizması. In: Proceedings of 12nd Meeting of Aktive Tectonic Research Group; Akçakoca-Düzce, Turkey. pp. 42-44 (in Turkish).

Demirtaş R, Tepeuğur E (2017). Bolvadin (Afyon) Merkez yerleşsim alaninda son 15 yıllık dönemde oluşmuş yüzey kırıklarının oluşum mekanizması. In: Proceedings of the ATAG-21, p11, Aktif Tektonik Araştırma Grubu Çalıştayı, Afyon, Turkey, 26-28 October 2017.

Duman TY, Elmacı H, Özalp S, Olgun Ş, Emre Ö (2013). First Palaeoseismological Results From Simav Fault Zone. 66th Geological Congress of Turkey, Ankara Turkey. Pp. 28-29.

Duman TY, Çan T, Emre Ö, Kadirioğlu FT, Başarır Baştürk N et al. (2018). Seismotectonic database of Turkey. Bulletin of Earthquake Engineering 16 (8): 3277-3316.

Emre Ö, Duman TY, Doğan A, Özalp S, Tokay F et al. (2003). Surface Faulting Associated with the Sultandağı Earthquake (Mw 6.5) of 3 February 2002, Southwestern Turkey. Seismological Research Letters 74 (4): 382-392.

Emre Ö, Duman TY, Özalp S, Olgun Ş, and Elmacı H (2011). Active Fault Map of Turkey (Scale 1:250,000), General Directorate of Mineral Research and Exploration Special Publication Series, Afyon (NJ 36-5) Quadrangle, serial number: 16. Ankara, Turkey: MTA.

Emre Ö, Duman TY, Özalp S, Şaroğlu F, Olgun Ş et al. (2018). Active fault database of Turkey. Bulletin of Earthquake Engineering 16 (8): 3229-3275.

Erdik M, Uckan E, Sesetyan K, Demircioğlu MB, Celep U et al. (2002). Feb.3, 2002 Sultandağı (Turkey) Earthquake. Report by the Department of Earthquake Engineering, Kandilli Observatory and Earthquake Research Institute, Boğaziçi University, İstanbul, Turkey (in Turkish).

Ergin K, Güçlü U, Uz Z (1967). A catalogue of earthquakes for Turkey and surrounding area (11AD to 1964AD). İstanbul Technical University, Publications, no. 24, 189.

Ergintav S, Çakır Z, Doğan U, Çetin S, Şentürk S et al. (2017). Aseismic slip and surface creep on the Hazar-Palu section of the East Anatolian Fault, Turkey, in AGU Fall Meeting: New Orleans, USA.

Giaccio B, Galadini F, Sposato A, Messina P, Moro M et al. (2002). Image processing and roughness analysis of exposed bedrock fault planes as a tool for palaeoseismological analysis: results from the Campo Felice fault (central Apennines, Italy). Geomorphology 49: 281-301

Gürboğa S (2013). 28 March 1970 Gediz earthquake fault, western Turkey: palaeoseismology and tectonic significance. International Geology Review 55 (10): 1191-1201.

Gürsoy H, Temiz H, Tatar O, Barka A (1997). Gediz grabeni güney kenarındaki güncel deformasyon verileri. II. İzmir ve Çevresinin Jeoteknik ve Deprem Sorunları Sempozyumu, Bildiri Özetleri, İzmir, Turkey. pp 14 (in Turkish).

Harris RA (2017). Large earthquakes and creeping faults. Reviews of Geophysics 55 (1): 169-198.

Holzer TL (1984). Ground failure induced by groundwater withdrawal from unconsolidated sediment. Reviews in Engineering Geology 6: 67-105.

Hreinsdóttir S, Bennett RA (2009). Active aseismic creep on the Alto Tiberina low-angle normal fault, Italy. Geology 27 (8): 683-686.

Imamoglu M, Kahraman F, Cakir Z, Balik-Sanli F (2019). Ground Deformation Analysis of Bolvadin (W. Turkey) by Means of Multi-Temporal InSAR Techniques and Sentinel-1 Data. Remote Sensing 11: 1069.

Kalafat D, Görgün E (2017). An example of triggered earthquakes in western Turkey: 2000–2015 Afyon-Akşehir Graben earthquake sequences. Journal of Asian Earth Sciences 146: 103-113.

Karabacak V, Altunel E, Çakır Z (2011). Monitoring aseismic surface creep along the North Anatolian Fault (Turkey) using ground-based LIDAR. Earth and Planetary Science Letters 304 (1-2): 64-70.

Kaymakcı N (2006). Kinematic development and palaeostress analysis of the Denizli Basin (Western Turkey): Implications of spatial variation of relative palaeostress magnitudes and orientations. Journal of Asian Earth Sciences 27: 207-222.

Koca MY, Sözbilir H, Uzel B (2011). An Investigation on the Causes of Deformations Formed Along the Sarıgöl Fault Zone. Journal of Geological Engineering 35 (2): 151-173.

Koçyiğit A (1984). Güneybatı Türkiye ve yakın dolayında levha içi yeni tektonik gelişim. Türkiye Jeoloji Kurumu Bülteni 27 (1): 1- 15 (in Turkish).

Koçyiğit A, Ünay E, Saraç G (2000). Episodic graben formation and extensional neotectonic regime in west Central Anatolia and the Isparta Angle: a case study in the Akşehir-Afyon Graben, Turkey. Geological Society of London Special Publication 173: 405-421.

Koçyiğit A, Özacar A (2003). Extensional neotectonic regime through the NE edge of outer Isparta Angle, SW Turkey: new field and seismic data. Turkish Journal of Earth Sciences 12: 67-90.

KOERI (Kandilli Rasathanesi ve Deprem Araştırma Enstitüsü) (2019). Recent Earthquakes in Turkey [online]. Website http://www.koeri.boun.edu.tr/scripts/lst5.asp [accessed 13 May 2019].

Lee JC, Angelier J, Chu H T, Hu JC, Jeng F et al. (2003). Active fault creep variations at Chihshang, Taiwan, revealed by creep meter monitoring, 1998–2001. Journal of Geophysical Research: Solid Earth 108(B11).

Melosh HJ (1980). Rheology of the earth: theory and observation. In: Physics of the Earth's Interior, Proceedings of the 1979 Enrico Fermi Summer School; Varena, Italy. pp. 318 - 336.

Mozafari N, Sümer Ö, Tikhomirov D, Ivy-Ochs S, Alfimov V et al. (2019). Holocene seismic activity of the Priene–Sazlı Fault revealed by cosmogenic 36Cl, Western Anatolia, Turkey. Turkish Journal of Earth Sciences 28: 410-437.

Nadeau RM, McEvilly TV (1999). Fault slip rates at depth from recurrence intervals of repeating microearthquakes. Science 285 (5428): 718-721.

Özalp S, Emre Ö, Duman TY, Törk K, (2011). Karapınar (Konya) yöresindeki çizgisel uzanımlı yer çatlaklarının kökeni üzerine palaeosismolojik bulgular. Aktif Tektonik Araştırma Grubu Onbeşinci Çalıştayı (ATAG-15), 19-22 Ekim 2011, Çukurova Üniversitesi, Bildiri Özleri Kitabı, 20-21, Karataş-Adana (in Turkish).

Özalp S, Emre Ö, Şaroğlu F, Özaksoy V, Elmacı H et al. (2018). Active fault segmentation of the Çivril Graben System and surface rupture of the 1 October 1995 Dinar earthquake (Mw 6.2), Southwestern Anatolia, Turkey. Journal of Asian Earth Sciences 166: 136-151.

Özden S, Kavak KŞ, Koçbulut F, Över S, Temiz H (2002). 2002.02. 03 Çay (Afyon) earthquakes. Geological Bulletin of Turkey 45: 49-56.

Özer N (2006). New information on earthquake history of the Aksehir-Afyon Graben System, Turkey, since the second half of 18th century. Natural Hazards and Earth System Sciences 6 (6): 1017-1023.

Özkaymak Ç (2015). Tectonic analysis of the Honaz Fault (western Anatolia) using geomorphic indices and the regional implications. Geodinamica Acta 27 (2-3): 110-129.

Özkaymak Ç, Sözbilir H, Uzel B, Akyüz HS (2011). Geological and palaeoseismological evidence for late Pleistocene-Holocene activity on the Manisa fault zone, western Anatolia. Turkish Journal of Earth Sciences 20: 449-474.

Özkaymak Ç, Yıldız A, Sarıkaya H, Başaran C, Dumlupınar İ et al. (2014). Bolvadin Fayı boyunca meydana gelen yüzey deformasyonları, Batı Anadolu-Türkiye. 18th Meeting of Active Tectonic Research Group; Muğla, Turkey. pp. 52 (in Turkish).

Özkaymak Ç, Sözbilir H, Tiryakioğlu İ. Baybura T (2017). Geologic, Geomorphologic and Geodetic Analyses of Surface Deformations Observed in Bolvadin (Afyon-Akşehir Graben, Afyon). Geological Bulletin of Turkey 60: 169-188.

Özkaymak Ç, Sözbilir H, Geçievi OM, Tiryakioğlu İ (2018). Palaeoseismology on the Bolvadin Fault: Evidence for Tectonic Creep in Afyon-Akşehir Graben, Western Anatolia. Geoscience 2018, International Conference on Geology and Earth Science Abstract Book (Int J Earth Sci 2018, 1:2) p.65, May 2-4, Rome, Italy

Papanikolaou ID, Roberts GP, Michetti AM (2005). Fault scarps and deformation rates in Lazio–Abruzzo, Central Italy: comparison between geological fault slip-rate and GPS data. Tectonophysics 408: 147-176.

Pavlides S, Caputo R (2004). Magnitude versus faults' surface parameters: quantitative relationships from the Aegean Region. Tectonophysics 380: 159-188.

Pınar N, Lahn E (1952). Türkiye Depremleri İzahlı Kataloğu. Bayındırlık Bakanlığı, Yapı ve İmar İşleri Reisliği, No. 6, Ankara, Turkey (in Turkish).

Poyraz F, Tatar O, Hastaoğlu KÖ, Tiryakioğlu İ, Gürsoy Ö et al. (2015). Gediz Grabeninin Doğu Kesimindeki Güncel Tektonik Hareketlerin GPS ve Ps-InSAR Yöntemleri Kullanılarak Belirlenmesi; İlk Sonuçlar. Harita Teknolojileri Elektronik Dergisi 7 (1): 17-28 (in Turkish).

Reimer PJ, Bard E, Bayliss A, Beck JW, Blackwell PG et al. (2013). IntCal13 and Marine13 radiocarbon age calibration curves 0–50,000 years cal BP. Radiocarbon 55 (4): 1869-1887.

Schulz SS, Mavko GM, Burford RO, Stuart WD (1982). Long-term fault creep observations in central California. Journal of Geophysical Research: Solid Earth 87(B8): 6977-6982.

Shebalin NV, Karnik V, Hadzievski D (1974). Catalogue of earthquakes of the Balkan region. I, UNDP-UNESCO Survey of the seismicity of the Balkan region. Skopje. pp 600.

Sieh KE, Williams PH (1990). Behavior of the southernmost San Andreas Fault during the past 300 years. Journal of Geophysical Research 95 (B5): 6629-6645.

Soysal H, Sipahioğlu S, Kolçak D, Altınok, Y (1981). Türkiye ve Çevresinin Tarihsel Deprem Kataloğu (2100 B.C.–1900 A.D.). TÜBİTAK raporu, No. TBAG-341 (in Turkish).

Stewart I (1996). A rough guide to limestone fault scarps. Journal of Structural Geology 18: 1259- 1264.

Tan O, Tapirdamaz MC, Yörük A (2008). The earthquakes catalogues for Turkey. Turkish Journal of Earth Sciences 17: 405-418.

Taymaz T, Tan O (2001). Source parameters of June 6, 2000 OrtaÇankırı (Mw = 6.0) and December 15, 2000 Sultandağı-Akşehir (Mw = 6.0) earthquakes obtained from inversion of teleseismic Pand SH- body-waveforms. Scientific Activities 2001 Symposia; İstanbul, Turkey. pp 96-107.

Thatcher W (1979). Systematic inversion of geodetic data in central California. Journal of Geophysical Research: Solid Earth 84 (B5): 2283-2295.

Tiryakioğlu I, Floyd M, Erdogan S, Gülal E, Ergintav S et al. (2013). GPS constraints on active deformation in the Isparta Angle region of SW Turkey. Geophysical Journal International 195: 1455-1463.

Tiryakioğlu İ, Baybura T, Özkaymak Ç, Sözbilir H, Sandıkçıoğlu A et al. (2015). Sultandağı Fayı Batı Kısmı Fay Aktivitelerinin Multidisipliner Çalışmalarla Belirlenmesi. Harita Teknolojileri Elektronik Dergisi 7 (1): 7-16 (in Turkish).

Tiryakioğlu İ, Özkaymak Ç, Baybura T, Sözbilir H, Uysal M (2018). Comparison of Palaeostress Analysis, Geodetic Strain Rates and Seismic Data in the Western Part of The Sultandağı Fault in Turkey. Annals of Geophysics 61 (3): GD335.

Tiryakioğlu İ, Yiğit CO, Özkaymak Ç, Baybura T, Yılmaz M et al., 2019. Active surface deformations detected by precise levelling surveys in the Afyon-Akşehir Graben, Western Anatolia, Turkey. Geofizika 36: 33-52.

Titus SJ, DeMets C, Tikoff B (2006). Thirty-five-year creep rates for the creeping segment of the San Andreas fault and the effects of the 2004 Parkfield earthquake: Constraints from alignment arrays, continuous global positioning system, and creepmeters. Bulletin of the Seismological Society of America 96 (4B): S250-S268.

Tong X, Smith-Konter, Sandwell DT (2014). Is there a discrepancy between geological and geodetic slip rates along the San Andreas Fault System. Journal of Geophysical Research: Solid Earth 119 (3): 2518-2538.

Tsodoulos IM, Stamoulis K, Caputo R, Koukouvelas I, Chatzipetros A et al. (2016). Middle-Late Holocene earthquake history of the Gyrtoni Fault, Central Greece: insight from optically stimulated luminescence (OSL) dating and palaeoseismology. Tectonophysics 687: 14-27.

Wang K (1995). Coupling of tectonic loading and earthquake fault slips at subduction zones. Pure and applied geophysics 145 (3-4): 537-559.

Wells DL, Coppersmith KJ (1994). New empirical relationship among magnitude, rupture length, rupture width, rupture area, and surface displacement. Bulletin of the Seismological Society of America 84: 974-1002.

Yürür T, Köse O, Demirbağ H, Özkaymak Ç, Selçuk L (2003). Could the coseismic fractures of a lake ice reflect the earthquake mechanism? (Afyon earthquakes of 2 February 2002, Central Anatolia, Turkey). Geodinamica Acta 16 (2-6): 83-87.